

## Groundwater Flow Field Distortion by Monitoring Wells and Passive Flux Meters

by G. Verreydt<sup>1,2</sup>, J. Bronders<sup>1</sup>, I. Van Keer<sup>1</sup>, L. Diels<sup>1,3</sup>, and P. Vanderauwera<sup>4</sup>

### Abstract

Due to differences in hydraulic conductivity and effects of well construction geometry, groundwater lateral flow through a monitoring well typically differs from groundwater flow in the surrounding aquifer. These differences must be well understood in order to apply passive measuring techniques, such as passive flux meters (PFMs) used for the measurement of groundwater and contaminant mass fluxes. To understand these differences, lab flow tank experiments were performed to evaluate the influences of the well screen, the surrounding filter pack and the presence of a PFM on the natural groundwater flux through a monitoring well. The results were compared with analytical calculations of flow field distortion based on the potential theory of Drost et al. (1968). Measured well flow field distortion factors were found to be lower than calculated flow field distortion factors, while measured PFM flow field distortion factors were comparable to the calculated ones. However, this latter is not the case for all conditions. The slotted geometry of the well screen seems to make a correct analytical calculation challenging for conditions where flow field deviation occurs, because the potential theory assumes a uniform flow field. Finally, plots of the functional relationships of the distortion of the flow field with the hydraulic conductivities of the filter screen, surrounding filter pack and corresponding radii make it possible to design well construction to optimally function during PFM applications.

### Introduction

The increasing interest in the in situ measurement of groundwater and contaminant mass fluxes emphasizes the importance of a good knowledge of the groundwater flow field surrounding and inside a monitoring well and through the flux measurement device. Indeed, subsurface contaminant mass flows and fluxes are increasingly being viewed as critical information needed for soil and groundwater remediation. Mass flux estimations are used for source and plume characterization and prioritization, compliance monitoring, remediation endpoint evaluation, natural attenuation assessment, and risk-based groundwater management (Schwarz et al. 1998; Einarson and Mackay 2001; Annable 2008; Brooks et al. 2008; Caterina et al. 2009; Brusseau et al. 2011; Swartjes 2011; Verreydt et al. 2012). The combined in situ measurement of contaminant mass fluxes and Darcy water fluxes in groundwater is

possible with the passive flux meter (PFM), a recently developed passive sampling device that is placed directly in a monitoring well or borehole where it intercepts the natural groundwater flow and captures contaminants (Hatfield et al. 2004; Annable et al. 2005). Natural groundwater fluxes however, are disturbed by the presence of a monitoring well and a PFM when applied. The distortion of a uniform flow field in a homogeneous aquifer depends on the hydraulic conductivities of the PFM, the well screen, the surrounding filter pack, and the aquifer, as well as on the thickness of the filter pack compared to the radius of the PFM (Klammler et al. 2007a). This study investigates the influences of these parameters by varying them in (1) an analytical simulation based on the potential flow field theory for open boreholes (Drost et al. 1968; Klammler et al. 2007b) and (2) a lab-scale flow through tank experimental setup. An important parameter for the evaluation is the flow distortion or convergence/divergence factor  $\alpha$  [-], which characterizes the magnitude of the distortion of the flow field. The distortion factor is defined as the degree of convergence or divergence of groundwater flow in the vicinity of the monitoring well with or without a PFM installed.

### Theory

The streamlines around a borehole or monitoring well, whether or not equipped with a PFM, will be

<sup>1</sup>Flemish Institute for Technological Research, Boeretang 200, B-2400 Mol, Belgium.

<sup>2</sup>Corresponding author: Department of Biology, University of Antwerp, Universiteitsplein 1C, B-2610 Antwerpen, Belgium; +32 3 265 23 04; fax: +32 3 265 22 71; goedele.verreydt@uantwerpen.be

<sup>3</sup>Department of Biology, University of Antwerp, Universiteitsplein 1C, B-2610 Antwerpen, Belgium.

<sup>4</sup>Department of Industrial Engineering, University of Antwerp, Salesianenlaan 30, B-2660 Hoboken, Belgium.

Received March 2014, accepted September 2014.

© 2015, National Ground Water Association.

doi: 10.1111/gwat.12290

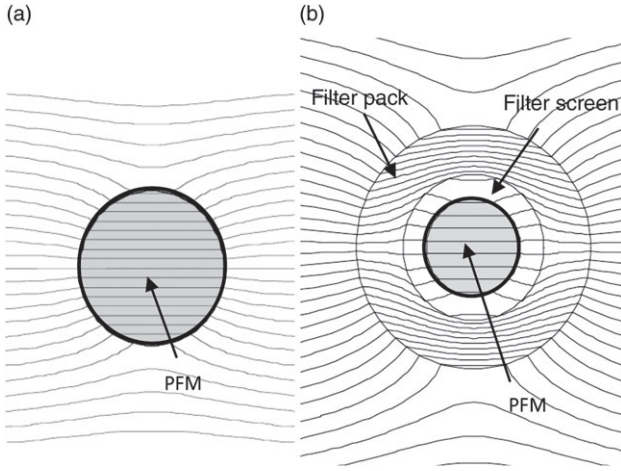


**Figure 1.** Converging and diverging flow lines in a uniform groundwater flow field due to the presence of (a) a borehole with a PFM installed and (b) a monitoring well with filter pack and PFM installed (after Klammler et al. 2007b).

disturbed because of the different hydraulic conductivities of the well filter, flux measurement device, and surrounding aquifer (Figure 1).

The water flux ( $q$ ) through the PFM or monitoring well [ $\text{m}^3/\text{m}^2/\text{day}$ ] is directly proportional to the water flux ( $q_0$ ) in the aquifer [ $\text{m}^3/\text{m}^2/\text{day}$ ]. This is expressed in Basu et al. (2006) and Börke (2007):

$$q_0 = \frac{q}{\alpha} \quad (1)$$

where  $\alpha$  is the convergence/divergence of the groundwater flow in the vicinity of a monitoring well with or without a PFM installed [-]. In case of an open monitoring well,  $\alpha$  can be calculated from the potential theory (Drost et al. 1968). If a monitoring well is equipped with a PFM,  $\alpha$  can be calculated from the adapted potential theory (Klammler et al. 2007b). **The potential theory assumes a uniform flow field in a homogeneous domain. In this lab study, vertical flows in the monitoring well and skin effects, caused by damage to the formation surrounding the well borehole, are not taken into account.** However, a potential impact of vertical flows and skin effects on the groundwater flux through monitoring wells in the field cannot be excluded (Kearl 1997; Elci et al. 2001; Clemo 2010; Vermeul et al. 2011).

### Monitoring Well Without Filter Pack in a Homogeneous Aquifer

The distortion of the groundwater flow passing a monitoring well with a single filter zone, without a filter pack, can be calculated according to the potential theory (Ogilvi 1958; Drost et al. 1968) as:

$$\alpha = \frac{4}{\left(1 + \frac{k_A}{k_S}\right) + \left(1 - \frac{k_A}{k_S}\right) \left(\frac{r_1}{r_2}\right)^2} \quad (2)$$

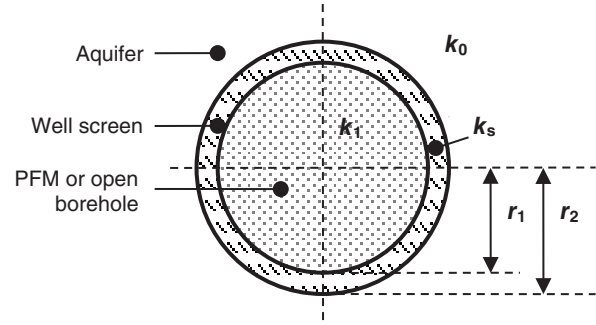


**Figure 2.** Monitoring well containing one concentric filter zone in a homogeneous aquifer ( $r_1$ : inside radius of well screen;  $r_2$ : outside radius of well screen;  $k_p$ : PFM hydraulic conductivity;  $k_s$ : well screen hydraulic conductivity;  $k_A$ : aquifer hydraulic conductivity).

where  $k_A$  and  $k_s$  represent the hydraulic conductivities of, respectively, the surrounding aquifer and the well filter screen,  $r_1$  and  $r_2$  indicate the corresponding distances to the center point of the monitoring well. Figure 2 shows a horizontal cross-section of the configuration and explains these parameters graphically.

If the PFM is placed in a monitoring well without surrounding filter pack,  $\alpha$  is calculated by (Klammler et al. 2007b):

$$\alpha = \frac{4}{\left(1 + \frac{k_A}{k_S}\right) \left(1 + \frac{k_S}{k_P}\right) + \left(1 - \frac{k_A}{k_S}\right) \left(1 - \frac{k_S}{k_P}\right) \left(\frac{r_1}{r_2}\right)^2} \quad (3)$$

where  $k_p$  represents the hydraulic conductivity of the PFM (Figure 2).

### Monitoring Well with Filter Pack in Homogeneous Aquifer

For a monitoring well containing two concentric filter zones (monitoring well with filter screen and surrounding filter pack), Equation 2 can be expanded as follows (Drost et al. 1968):

$$\alpha = \frac{8}{\left(1 + \frac{k_A}{k_F}\right) \left( \left[1 + \left(\frac{r_1}{r_2}\right)^2\right] + \frac{k_F}{k_S} \left[1 - \left(\frac{r_1}{r_2}\right)^2\right] \right) + \left(1 - \frac{k_A}{k_F}\right) \left[ \left(\frac{r_1}{r_3}\right)^2 + \left(\frac{r_2}{r_3}\right)^2 \right] + \left(\frac{k_F}{k_S}\right) \left[ \left(\frac{r_1}{r_3}\right)^2 - \left(\frac{r_2}{r_3}\right)^2 \right]} \quad (4)$$

where  $k_F$  represents the hydraulic conductivity of the gravel filter surrounding the monitoring well,  $r_3$  indicates the corresponding distance to the center point of the monitoring well (Figure 3).

If the PFM is placed in a monitoring well with surrounding filter pack,  $\alpha$  can be calculated by

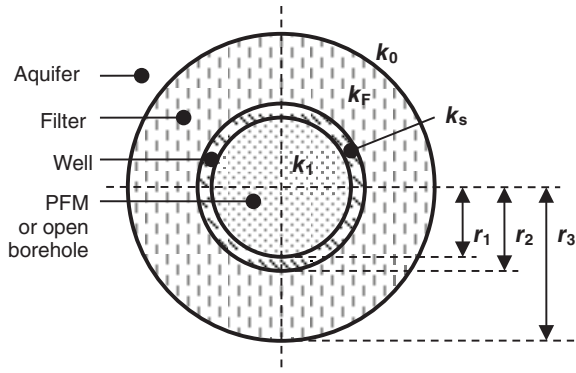


**Figure 3. Monitoring well containing two concentric filter zones in a homogeneous aquifer ( $r_1$ : inside radius of well screen;  $r_2$ : outside radius of well screen;  $r_3$ : outside radius of the gravel filter pack;  $k_p$ : PFM hydraulic conductivity;  $k_s$ : well screen hydraulic conductivity;  $k_F$ : hydraulic conductivity of filter pack;  $k_A$ : aquifer hydraulic conductivity).**

(Klammler et al. 2007b):

$$\alpha = \frac{8}{\left(1 + \frac{k_A}{k_F}\right) \left(1 + \frac{k_F}{k_S}\right) \left(1 + \frac{k_S}{k_P}\right) + \left(1 - \frac{k_A}{k_F}\right) \left(1 - \frac{k_F}{k_S}\right) \left(1 + \frac{k_S}{k_P}\right) \left(\frac{r_2}{r_3}\right)^2 + \left(1 + \frac{k_A}{k_F}\right) \left(1 - \frac{k_F}{k_S}\right) \left(1 - \frac{k_S}{k_P}\right) \left(\frac{r_1}{r_2}\right)^2 + \left(1 - \frac{k_A}{k_F}\right) \left(1 + \frac{k_F}{k_S}\right) \left(1 - \frac{k_S}{k_P}\right) \left(\frac{r_1}{r_3}\right)^2} \quad (5)$$

## Materials and Methods

### Passive Flux Meter

The PFM is a passive sampler that provides simultaneous in situ point measurements of a time-averaged contaminant mass flux,  $J_c$ , and water flux,  $q_0$  (Hatfield et al. 2004; Annable et al. 2005; Basu et al. 2006). The PFM is typically placed in a monitoring well where it intercepts the groundwater flow and captures the contaminants. The PFM consists of a permeable sock which is packed with a permeable sorbent matrix (Figure 4). Each PFM has a diameter equal to the internal diameter of the selected monitoring well. Rubber washers are used inside the PFM to prevent vertical water flow and to make a vertical flux differentiation possible. A center tube serves as a backbone for the PFM and facilitates the installation and retrieval allowing water bypass. The PFMs made for this lab tank experiment were dimensioned at a length of 30 cm and consisted of three vertical segments. The sorbent matrix is impregnated with known amounts of one or more water soluble resident tracers. These tracers are leached from the PFM at rates proportional to the Darcy groundwater flux.

The water flux through a PFM, installed in well or borehole, can be calculated based on the tracer elution

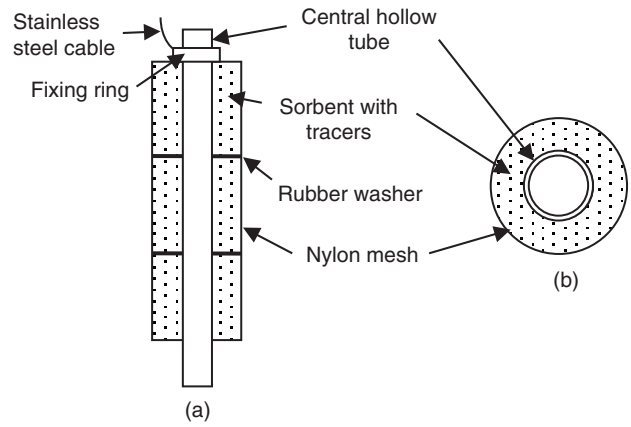


**Figure 4. (a) Vertical cross-section and (b) horizontal cross-section of a PFM.**

characteristics by (Hatfield et al. 2004):

$$q_{PFM} = \frac{1.67 \cdot r \cdot R_d \cdot (1 - \Omega_R)}{t} \quad (6)$$

where  $r$  is the radius of the PFM cylinder [m],  $R_d$  is the retardation coefficient [-] of the resident tracer on the sorbent (Hatfield et al. 2004; Appelo and Postma 2007),  $\Omega_R$  is the relative mass [-] of the resident tracer remaining in the PFM sorbent at the particular well depth, and  $t$  is the measurement time [day].

Subsequently, the Darcy groundwater flux through the surrounding aquifer based on PFM measurements can be calculated by Equation 1 where  $q = q_{PFM}$ .

It should be recognized that a PFM has in fact an impermeable center tube (Figure 4) and therefore Equations 3 and 5 are based on a simplification. Klammler et al. (2007b), however, compared the properties of a uniform flow field disturbed by an impermeable center tube to the case of a uniform flow in a circular flow domain and established this simplification.

### Lab Scale Flow-Through Tank

A plastic flow-through tank in the lab (Figure 5a; analogous to Kearn 1997; Graw et al. 2000; Labaky et al. 2007; Wu et al. 2008) was used to conduct experiments to determine the distortion of the groundwater flow field in the vicinity of a monitoring well under varying well diameter, well screen conductivity, filter pack material and presence of a PFM. The flow-through tank measures 82 cm in length, 72 cm in width and 62 cm in height, and is filled with high quality fractionized fine silica sand that is very homogeneous. The sand tank is filled under saturated conditions, to avoid air entrapment and layering. The sand properties are determined by sieve analysis, permeameter tests, volumetric moisture experiments and drying analysis (Sibelco M30, Table 1).

The size of the sand tank was designed to at least 10 times the radius of the largest well tube to avoid the effect of boundary conditions (Momii et al. 1993; Wu et al. 2008). The tank is equipped with screened baffle plates, coated with nylon mesh material, separating

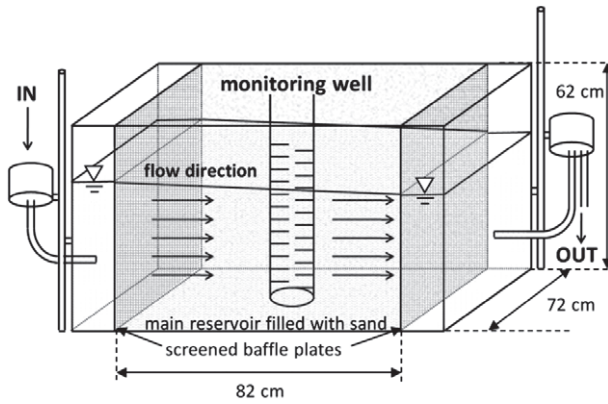


Figure 5. Lab-scale flow tank.

**Table 1**  
Characteristics of Sibelco M30 Sand

Parameter	Value
Mean grain size [mm]	0.32
Hydraulic conductivity [m/day]	$3.7 \times 10^{-04}$
Intrinsic permeability [ $\text{cm}^2$ ]	$3.78 \times 10^{-07}$
Bulk density [ $\text{g}/\text{cm}^3$ ]	1.7
Grain density [ $\text{g}/\text{cm}^3$ ]	2.61
Total porosity [%]	36.42
TOC [%]	0
Saturated water content [%]	36.42
Air dry water content [%]	0.072

the sand from the reservoirs at both ends of the tank (Figure 5b). The water flux through the sand tank has been realized by creating a hydraulic head difference  $\Delta h$  between the inflow and outflow reservoirs. During the test, the hydraulic gradient was controlled using the constant-head method through the drainage hole in two small water reservoirs, connected at both end reservoirs behind the screened baffle plates. Successively, different types of monitoring well filters were placed in the middle of the sand tank, surrounded by different filter pack grain sizes.

### Experimental Methodology

In this study, 10 sets of lab experiments were conducted under controlled flow conditions to evaluate the difference between flows in monitoring wells, with different types and sizes of filter screens and filter packs, flows in PFMs installed in these wells, and flows in the surrounding porous aquifer sand (Table 2). Five parameters—well screen diameter, slot size, filter pack presence and diameter, and grain size of filter sand—were varied in the sand tank tests. The average saturated thickness in the monitoring well is 45.7 cm. The experiments were performed at temperatures ranging from 12°C to 15°C which is slightly higher than common groundwater temperatures.

The difference in flow in the monitoring wells and installed PFMs vs. flow in the surrounding aquifer

sand is expressed as the convergence/divergence factor  $\alpha$  (Equation 1). For every experimental set, the  $\alpha$ -factors for the monitoring well with and without PFM installed are determined. The determination of the  $\alpha$ -factor is performed (1) through Equations 2 to 5, based on the hydraulic conductivities of the aquifer sand, well screen and filter pack and (2) by applying Equation 1 and measuring the flow in (a) the monitoring well through borehole dilution tests (Havely et al. 1967; Drost et al. 1968; Lamontagne et al. 2002; Massey et al. 2007; Pitrak et al. 2007) and (b) the PFM based on the PFM tracer elution characteristics (Equation 6). The hydraulic conductivities of the aquifer sand and filter sand are determined in the lab by permeameter experiments (Klute 1986; Eijkelkamp 2008). The hydraulic conductivities of the filter screens are known from the supplier (by Falling head method, Eijkelkamp Agrisearch Equipment, the Netherlands) and have been experimentally determined by borehole dilution tests. Water was circulated within the well during the borehole dilution test. The recirculation system consisted of a peristaltic pump (Eijkelkamp model 12Vdc), an inline injection port for the tracer salt solution (KBr) and a conductivity logger (CTD diver, Schlumberger Water Services) which was installed in the monitoring well. The system was designed for the well water to be circulated from the bottom to the top of the well at a rate of approximately one bore volume per minute. The background conductivity was recorded and stabilized before every borehole dilution test. After tracer injection ( $\pm 4 \text{ g/L}$  KBr in the monitoring well), the tracer concentration in the well is observed vs. time (Figure 7). To estimate the groundwater flow  $q$  in the well, a series of characteristic curves are plotted along with the standardized curve from the borehole dilution test (Equation 7) (Freeze and Cherry 1979):

$$C_{(t)}^* = e^{-\frac{q \cdot A \cdot t}{V}} \quad (7)$$

where  $A$  is the cross-section area of the water filled portion of the monitoring well [ $\text{cm}^2$ ],  $t$  the elapsed time [s], and  $V$  the total volume of recycled water through the monitoring well [ $\text{cm}^3$ ].

Several curves are plotted for different values of  $q$  until a reasonable match is available to compare with the experimental data. Subsequently, the hydraulic conductivity of the monitoring well filter  $k_{well}^*$  (including screen and filter pack) was calculated by extracting  $k_s$  from Equation 3. Hereby, parameter  $r_2$  stands for the outer radius of the well filter, including filter pack if present.

### Results and Discussion

The borehole dilution experiments in the monitoring wells produced smooth and reproducible results as shown in Figure 6.

Moreover, the repetition of set 3 (set 6) yielded exactly the same  $\alpha$ -factor, in spite of the new well installation, sand tank filling, and flow equilibration.

**Table 2**  
Characteristics of the Experimental Set-Ups

Set	Well ID [mm]	Well OD [mm]	Well Slot Size [mm]	$k_{screen}$ [m/s]	Filter Pack OD [mm]	Filter Sand $\emptyset$ [mm]	$k_{filter\ sand}$ [m/s]	$\Delta h$ [m]	Outflow [L/h]
1	104	114	0.3	0.09	120	0.75	0.1344	0.007	3.178
2	104	114	0.3	0.09	—	—	—	0.007	3.178
3	80	90	1.0	0.30	120	2.4–3.2	0.3966	0.007	3.178
4	80	90	1.0	0.30	120	1.2–2.4	0.1115	0.007	3.178
5	80	90	0.3	0.09	120	1.2–2.4	0.1115	0.007	3.242
6	80	90	1.0	0.30	120	2.4–3.2	0.3966	0.006	2.196
7	80	90	0.3	0.09	120	0.75	0.1344	0.006	1.950
8	80	90	0.3	0.09	—	—	—	0.007	2.928
9	41	50	0.3	0.09	100	1.2–2.4	0.1115	0.007	2.819
10	41	50	0.3	0.09	—	—	—	0.007	2.687



ID, inner diameter; OD, outer diameter;  $\emptyset$ , diameter;  $\Delta h$ , hydraulic head difference between in and outflow reservoir.

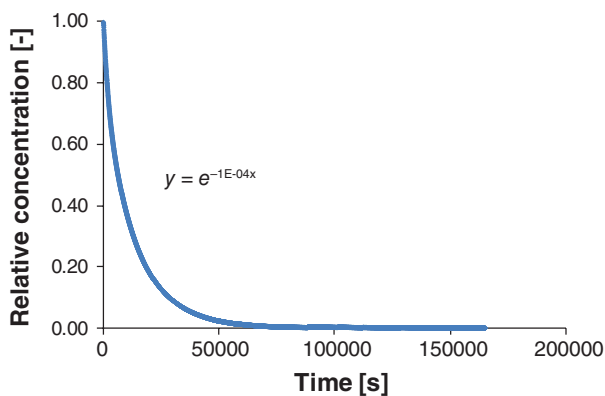


**Figure 6.** Borehole dilution test result of test set 7 ( $q_{A.V-1} = 0.0001$  cm/s)

Table 3 presents the measured groundwater velocities in the lab flow tank experiment.  $q_{Darcy}$  is calculated based on the hydraulic head difference between in and end reservoir,  $q_{outflow}$  is measured directly at the outflow of the end reservoir,  $q_{BD}$  is measured by performing a borehole dilution test in the monitoring well without PFM,  $q_{PFM}$  is calculated from Equation 6 after PFM exposure in the monitoring well. Table 4 comprises the (1) measured  $\alpha$ -factors, (2) the analytically calculated  $\alpha$ -values and effective hydraulic conductivities of the well filters ( $k^*_{well}$ , from Equation 2 where  $\alpha = \alpha_{well}$ ), and (3) an extra analytical  $\alpha$ -factor calculation for a well including a PFM, based on measured effective well filter hydraulic conductivities ( $k^*_{well}$ ). The latter supposes a simplification of the well filter into a conceptual model as shown in Figure 3, where the well screen may include the surrounding filter pack.

The well flow distortion ranged between 1.1 and 2.1 (Figure 7a). The real well flow distortion seemed to be lower than the calculated well flow distortion if no surrounding filter pack was present (Figure 8a). The effective well filter hydraulic conductivities were found to be much lower than the theoretical ones. Aquifer sand or even filter sand particles might have locally sealed

**Table 3**  
Measured Water Velocities in Lab Flow Tank

Set	$q_{Darcy}$ [cm/d]	$q_{outflow}$ [cm/d]	$q_{BD}$ [cm/d]	$q_{PFM}$ [cm/d]	$q_{PFM}/q_{BD}$ [-]
1	26.1	23.2	44.8	24.2	0.5
2	26.1	23.2	48.1	18.7	0.4
3	26.1	23.2	30.2	9.9	0.5
4	26.1	23.2	33.6	10.2	0.4
5	26.1	23.6	25.3	14.2	0.6
6	22.4	16.0	20.8	11.9	0.5
7	22.4	17.0	22.1	11.5	0.5
8	26.1	21.4	36.1	11.3	0.3
9	26.1	20.6	24.3	12.2	0.5
10	26.1	19.6	27.0	4.4	0.2

BD, borehole dilution test.

the well screen slots and lowered the effective hydraulic conductivity of the well screen. The PFM exposures in the flow tank yielded consistent results.

However, a discrepancy is observed between calculated  $\alpha$ -values based on Equations 3 to 5, and calculated  $\alpha$ -values based on the simplified approach using measured  $k^*_{well}$  values (Figure 8b). The simplified concept approach of the well filter geometry and conductivity (expressed in  $\alpha_{PFM}$  calculated from  $k^*_{well}$ ) seems the less correct since it notes the highest differences with the measured  $\alpha_{PFM}$ -values. Clearly a PFM installation also has an impact on the effective hydraulic conductivity of the well screen. Figure 7b shows the distribution of the  $\alpha$ -factors of the water flow through the PFM in the different test sets. PFMs installed in wells without filter packs are associated with lower  $\alpha$ -factors. Low calculated  $\alpha_{PFM}$ -factors on the other hand, are not always associated with low measured  $\alpha_{PFM}$  factors (Figure 8b).

As it is important for the interpretation of the measured flux results to understand the influences of the hydraulic conductivities of the well screen, well filter pack and corresponding radii on the water flux through a PFM, an analytical analysis of these parameters has additionally been performed by drawing the functional

**Table 4**  
**Measured and Calculated  $\alpha$ -Factors from Lab Flow Tank Experiment**

Set	$\alpha_{\text{well}}$ Measured = $q_{\text{BD}}/q_{\text{outflow}}$ [-]	$\alpha_{\text{well}}$ Calculated (Equations 2 and 4) [-]	$\alpha_{\text{PFM}}$ Measured = $q_{\text{PFM}}/q_{\text{outflow}}$ [-]	$\alpha_{\text{PFM}}$ Calculated (Equations 3 and 5) [-]	$k^*_{\text{well}}$ (Equation 2) [m/s]	$\alpha_{\text{PFM}}$ Calculated from $k^*_{\text{well}}$ (Equation 3) [-]
1	1.93	1.74	1.05	0.70	$2.8 \times 10^{-4}$	1.78
2	2.08	2.18	0.81	0.68	$6.2 \times 10^{-4}$	1.88
3	1.30	1.27	0.63	0.25	$1.2 \times 10^{-4}$	1.24
4	1.45	1.28	0.64	0.27	$1.5 \times 10^{-4}$	1.37
5	1.07	1.28	0.60	0.67	$0.9 \times 10^{-4}$	1.03
6	1.30	1.27	0.67	0.25	$1.2 \times 10^{-4}$	1.24
7	1.30	1.28	0.68	0.68	$1.2 \times 10^{-4}$	1.24
8	1.69	2.23	0.53	0.58	$1.3 \times 10^{-4}$	1.58
9	1.18	0.91	0.59	0.58	$1.2 \times 10^{-4}$	1.08
10	1.38	2.39	0.23	0.42	$0.9 \times 10^{-4}$	1.30

$k^*_{\text{well}}$  is calculated from Equation 2 were  $\alpha = \alpha_{\text{well}}$  and  $k^*_{\text{well}} = k_S$ ; BD, borehole dilution test.

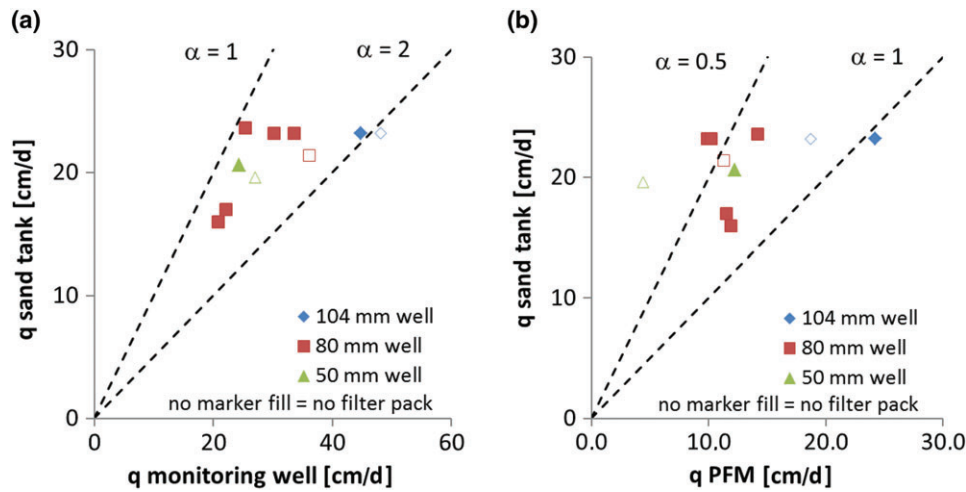


**Figure 7. Distribution of the flow convergence/divergence factors obtained in the test sets, in (a) monitoring well and (b) monitoring well with PFM installed.**

relationships of these parameters with the  $\alpha$ -factor. As suggested by H. Klammler (personal communication, February 12, 2009) Equations 3 and 5 are transformed in terms of relative conductivities and radii of well screen, well filter pack and PFM. Hence, this transformation uses  $K_D$  [-] for  $k_P/k_A$  to represent the dimensionless conductivity of the PFM,  $K_S$  [-] for  $k_S/k_A$  to characterize the dimensionless conductivity of the well screen,  $K_F$  [-] for  $k_F/k_0$  to count for the dimensionless conductivity of the filter pack, and  $R_S$  [-] and  $R_F$  for respectively  $r_2/r_1$  and  $r_3/r_1$ . These substitutions normalize the problem to the case of an aquifer of conductivity 1 with a PFM of radius 1 surrounded by a well screen and filter pack.

#### Influences of Hydraulic Conductivity of Well Screen and Filter Pack

The two most uncertain parameters in the calculation of the  $\alpha$ -factor are the hydraulic conductivities of the well screen and surrounding filter pack. Both parameters are difficult to determine, very sensitive to the well

field installation characteristics and can be influenced by fouling or clogging. The plots of  $\alpha_{\text{PFM}}$  as a function of the dimensionless hydraulic conductivity of the PFM ( $K_D$ ) and the filter screen ( $K_S$ ) for respectively a monitoring well without and with surrounding filter pack are given in Figure 9a and 9b. The fixed parameters  $R_S$ ,  $R_F$ , and  $K_F$  are average values from the experimental test sets (see Table 2).

The plots of  $\alpha_{\text{PFM}}$  as a function of  $K_S$  and  $K_F$  for a monitoring well with filter pack are presented in Figure 10a, 10b, and 10c for respectively three different values of  $K_D$ .

It can be seen from Figure 9 that the  $\alpha$ -factor will decrease again if a certain  $K_S$  value has been reached. Considering realistic  $K_D$  values ranging between 10 and 1000,  $\alpha$  will decrease if a  $K_S$  value of respectively 10 and 500 has been exceeded. The phenomenon is presumably due to the increasing effects of flow bypass through the highly permeable filter screen. However, this effect is not noticed in the lab tank experiments. Increasing

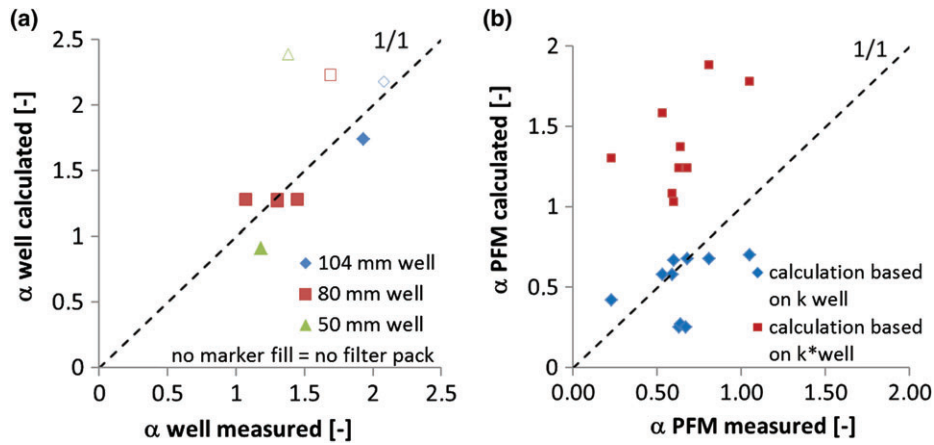


Figure 8. Comparison between the calculated and measured  $\alpha$  factors, in (a) monitoring well, and (b) monitoring well with PFM installed.

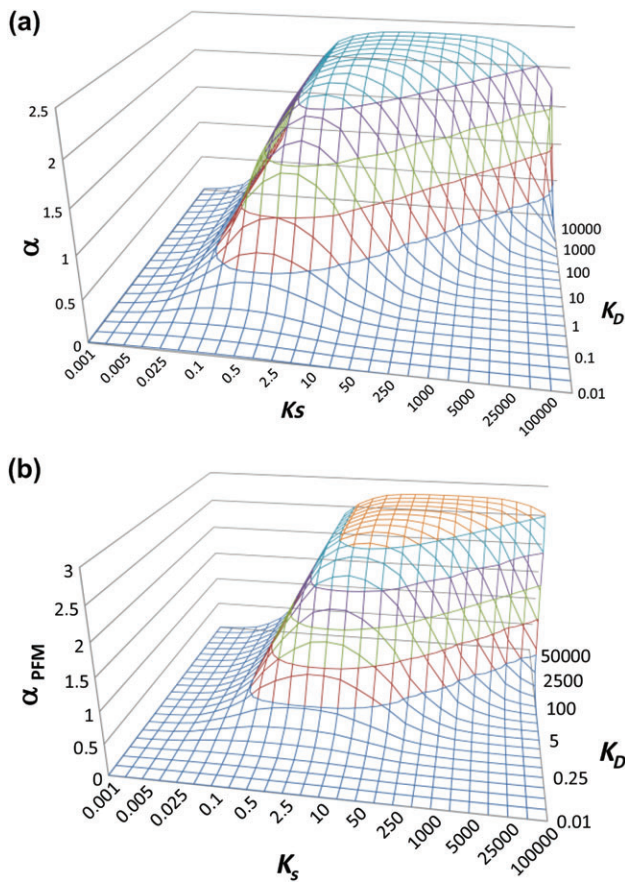


Figure 9.  $\alpha$  as a function of  $K_S$  (filter screen) and  $K_D$  (PFM) for (a) a monitoring well without filter pack ( $R_S = 1.1$ ) and (b) a monitoring well with filter pack ( $R_S = 1.1$ ,  $R_F = 1.5$ , and  $K_F = 12$ ).

$k_s$ —and thus also  $K_S$ -values—does not seem to have an impact at all (Figure 11).

The reason for this may be found in the well screen geometry. The geometry of the well screen does not allow complete flow bypass as it is slotted. A range of horizontal slots or cuts in the well tube define the screen area. Therefore, the potential theory should in fact not be

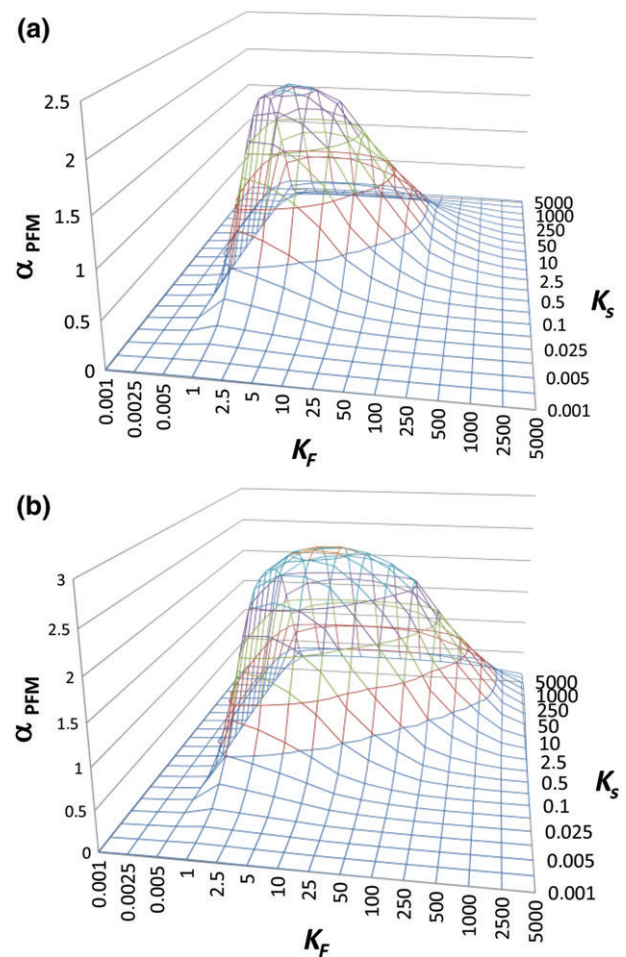
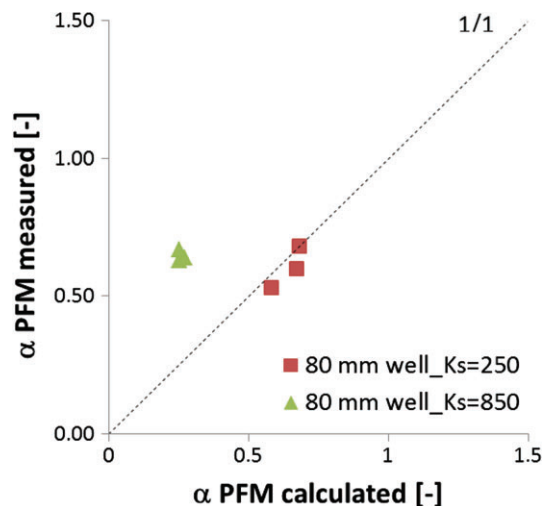


Figure 10.  $\alpha$  as a function of  $K_F$  and  $K_S$  for a monitoring well with filter pack ( $R_S = 1.1$ ,  $R_F = 1.5$ ) and for (a) a  $K_D$  of 10 and (b) a  $K_D$  of 1000.

applied because the filter screen is not a porous medium allowing a homogeneous flow field. Anyway, it is always advantageous to select for a combination of  $K_S$  and  $K_D$  where  $\alpha$  approaches its maximum. Under this scenario  $\alpha$  becomes less sensitive to variations with  $K_S$ , and potential



**Figure 11.**  $\alpha$  relation with well screen hydraulic conductivity ( $R_S = 1.1$ ,  $R_F = 1.5$ ,  $K_D = 10$ , and  $K_F = 12$ ).

incorrect estimations of  $K_S$  have lower impact on the end result. It can be seen from Figure 10 that  $K_F$  has a similar influence on the  $\alpha$ -factor as  $K_S$ . The area of independency of  $\alpha$  from both  $K_S$  and  $K_F$  increases as  $K_D$  increases.

### Influences of Well Screen and Filter Pack Radii

The analytical relationships between the flow convergence/divergence factor through a PFM and the well screen and filter pack radii, based on Equation 5, are presented in Figure 12. The  $\alpha$ -factor decreases with increasing filter screen thickness (Figure 12a). The influence of the filter pack thickness on the  $\alpha$ -factor is minor (Figure 12b). These effects are not clearly noticed in the flow tank experiments. The flow tank test sets did point out a significant increase of the  $\alpha$ -factor with increasing well diameter (Figure 8). The latter cannot be proved by drawing relative functional relationships of  $\alpha$ .

### Conclusions

The influences of a well filter, surrounding filter pack and presence of a PFM on the natural water flux through a monitoring well have been investigated in lab flow

tank experiments and by analytical modeling based on the potential theory of Drost et al. (1968).

The lab flow tank experiments resulted in the determination of a distortion factor  $\alpha$  of the water flow through the monitoring well ranging from 0.9 to 2.4 for the different well constructions, including well screen diameter, slot size and filter pack characteristics. Effective well filter hydraulic conductivities are found to be lower than the theoretical ones. The same well conditions yielded lower  $\alpha$ -factors of the water flow if PFMs were installed, ranging from 0.2 and 1.1. Since the  $\alpha$ -factors do not always approximate the value 1, it is important to correctly estimate this factor and take it into account when determining aquifer fluxes.

Generally, similarities between the calculated and the measured  $\alpha$ -values were observed. However, this is not the case for all conditions. The simplified concept approach of the well filter geometry and conductivity (expressed in  $\alpha_{\text{PFM}}$  calculated based on  $k^*$ well) seems the less robust since it notes the highest differences with the measured  $\alpha_{\text{PFM}}$ -values. PFM installation influences the well screen hydraulic conductivity. Also, the slotted geometry of the well screen makes a correct calculation based on the potential theory impossible since a uniform flow field cannot be guaranteed in all conditions. Complete flow bypass through the well screen, as assumed in the potential theory of Drost et al. (1968), can never take place. Numerical simulation can be used instead of the potential theory of Drost et al. (1968), or the hydraulic conductivity of the well screen in the potential theory formula should be reduced to the value of the PFM hydraulic conductivity. The influence of the well screen conductivity seems to be negligible once a minimum hydraulic conductivity has been reached.

The plots of the functional relationships of  $\alpha$  with the hydraulic conductivities of the filter screen, surrounding filter pack and corresponding radii, calculated by a normalization of the potential flow field theory, made it possible to delineate an optimum design of a well in function of a PFM application:

- The PFM hydraulic conductivity should be at least three times the filter pack hydraulic conductivity.

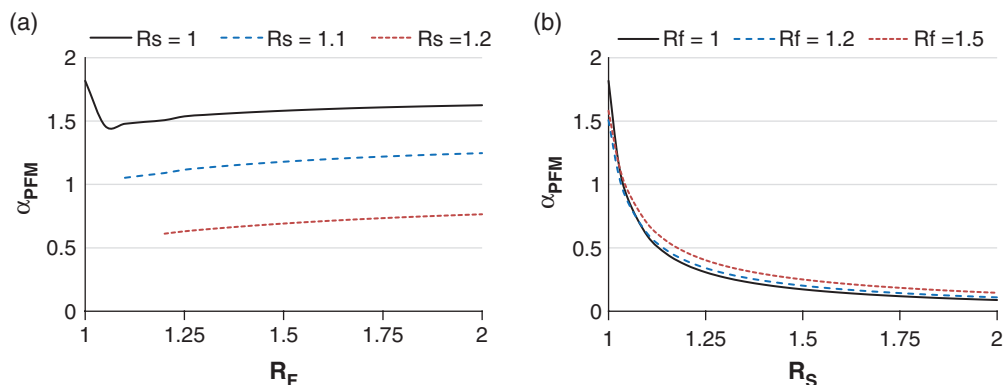


**Figure 12.**  $\alpha$  for a PFM placed in a monitoring well ( $K_D = 10$ ,  $K_S = 250$ , and  $K_F = 12$ ) as a function of (a)  $R_S$  and (b)  $R_F$ .



- A well slot size of 0.3 mm provides sufficient flow. If higher slot sizes are used, the potential theory may be not applied for calculation due to the flow bypass effect of an assumed homogeneous screen.
- The ratio of the filter pack radius vs. the PFM radius has proven to produce reliable results within a range of 1.1 to 1.5.

### Recommendations and Perspectives

This study has proven the importance of investigating the influence of well characteristics and PFM deployment on the natural water flux through a groundwater monitoring well. Real conditions often differ from theoretical conditions. It is very important to know the real flow convergence/divergence in order to calculate aquifer fluxes from measured fluxes. It is recommended that monitoring wells are screened prior to the installation of PFMs in order to make sure that all conditions are met for a reliable  $\alpha$ -factor determination. Also, PFM and well optimization may be performed based on the results of this study.

### Acknowledgments

This study is part of the PhD research of Goedele Verreydt and funded through the Flemish Institute for Technological Research (VITO NV). Mr. Andrew J. Victor is gratefully acknowledged for the linguistic improvements.

### References

Annable, M.D. 2008. Mass flux as a remedial performance metric at NAPL contaminated sites. In *Methods and Techniques for Cleaning Up Contaminated Sites*. NATO Science for Peace and Security Series C—Environmental Security, 177–186. the Netherlands: Springer.

Annable, M.D., K. Hatfield, J. Cho, H. Klammler, B.L. Parker, J.A. Cherry, and P.S.C. Rao. 2005. Field-scale evaluation of the passive flux meter for simultaneous measurement of groundwater and contaminant fluxes. *Environmental Science & Technology* 39, no. 18: 7194–7201.

Appelo, C.A.J., and D. Postma. 2007. *Geochemistry, Groundwater and Pollution* (2nd Reprint with corrections), ed. Amsterdam, The Netherlands: A.A. Balkema.

Basu, N.B., P.S.C. Rao, I.C. Poyer, M.D. Annable, and K. Hatfield. 2006. Flux-based assessment at a manufacturing site contaminated with trichloroethylene. *Journal of Contaminant Hydrology* 86: 105–127.

Börke, P. 2007. Untersuchungen zur Quantifizierung der Grundwasserimmission vor Polyzyklischen Aromatischen Kohlenwasserstoffen mithilfe von Passiven Probennahmesystemen (in German). PhD dissertation, Technische Universität Dresden, Dresden, Germany.

Brooks, M.C., A.L. Wood, M.D. Annable, K. Hatfield, J. Cho, C. Holbert, P.S.C. Rao, C.G. Enfield, K. Lynch, and R.E. Smith. 2008. Changes in contaminant mass discharge from DNAPL source mass depletion: evaluation at two field sites. *Journal of Contaminant Hydrology* 102: 140–153.

Brusseau, M.L., K.C. Carroll, T. Allen, J. Baker, W. DiGuseppi, J. Hatton, C. Morrison, A. Russo, and J. Berkompas. 2011. Impact of in situ chemical oxidation on contaminant mass discharge: linking source-zone and plume-scale characterizations of remediation performance. *Environmental Science and Technology* 45, no. 12: 5352–5358.

Caterina, D., S. Brouyère, P. Jamin, J. Batlle-Aguilar, A. Dassargues, W. Dejonghe, L. Diels, S. Crèvecoeur, J.-P. Thomé, J. Dujardin, O. Batelaan, F. Canters, and C. Hérivaux. 2009. Flux-based risk assessment of the impact of contaminants on water resources and ecosystems (FRAC-WECO). Final Report. Belgian Science Policy 2009, Brussels (Research Programme Science for a Sustainable Development).

Clemo, T. 2010. Coupled aquifer-borehole simulation. *Ground Water* 48, no. 1: 68–78.

Drost, W., D. Klotz, A. Koch, J. Moser, F. Neumaier, and W. Rauert. 1968. Point dilution method measuring groundwater flow by means of radioisotopes. *Water Resources Research* 4: 125–146.

Eijkelkamp. 2008. Operating Instructions 09.02 Laboratory permeameter. M1.09.02.E.

Einarson, M.D., and D.M. Mackay. 2001. Predicting the impacts of groundwater contamination. *Environmental Science and Technology* 35, no. 3: 66A–73A.

Elci, B.A., F.J. Molz, and W.R. Waldrop. 2001. Implications of observed and simulated ambient flow in monitoring wells. *Ground Water* 39, no. 6: 853–862.

Freeze, R.C., and J.A. Cherry. 1979. *Groundwater*. Englewood Cliffs, NJ: Prentice-Hall Inc.

Graw, K.-U., N. Jagsch, J. Lengricht, H. Storz, and J. Schöne. 2000. Comprehension of borehole flow for groundwater flow information. *12th Conference of the Asia and Pacific Regional Division of the IAHR*, Bangkok, 13–15 November.

Hatfield, K., M.D. Annable, J. Cho, P.S.C. Rao, and H. Klammler. 2004. A direct passive method for measuring water and contaminant fluxes in porous media. *Journal of Contaminant Hydrology* 75: 155–181.

Havelly, E., H. Moser, O. Zellhofer, and E. Zuber. 1967. Borehole dilution techniques: A critical review. In *Isotopes in Hydrology*, 531–564. Vienna, Austria: I.A.E.A.

Kearl, P.M. 1997. Observations of particle movement in a monitoring well using the colloidal borescope. *Journal of Hydrology* 200: 323–344.

Klammler, H., K. Hatfield, and M.D. Annable. 2007a. Concepts for measuring horizontal groundwater flow directions using the passive fluxmeter. *Advances in Water Resources* 30: 984–997.

Klammler, H., K. Hatfield, M.D. Annable, E. Agyei, B.L. Parker, J.A. Cherry, and P.S.C. Rao. 2007b. General analytical treatment of the flow field relevant to the interpretation of passive fluxmeter measurements. *Water Resources Research* 43: W04407. DOI:10.1029/2005WR004718.

Klute, A. 1986. *Methods of Soil Analysis, Part 1: Physical and Mineralogical Methods*. SSSA Book Series: 5. Madison, Wisconsin: American Society of Agronomy, Inc.

Labaky, W., J.F. Devlin, and R.W. Gillhams. 2007. Probe for measuring groundwater velocity at the centimeter scale. *Environmental Science & Technology* 41: 8453–8458.

Lamontagne, S., J. Dighton, and W. Ullman. 2002. Estimates of groundwater velocity in riparian zones using point dilution tests. CSIRO Technical Report 14/02, Glenn Osmond, Australia, pp. 16.

Massey, A.J., P.J. Friesz, and C.S. Carlson. 2007. Borehole-dilution tests to measure natural flushing of screens in wells monitored with passive diffusion sampling. USGS Report 48-10. Northborough, Massachusetts: U.S. Geological Survey.

Momii, K., K. Jinno, and F. Hirano. 1993. Laboratory studies on a new laser Doppler velocimeter system for horizontal groundwater velocity measurements in a borehole. *Water Resources Research* 29, no. 2: 283–291.

Ogilvi, N.A. 1958. An electrolytical method of determining the filtration velocity of underground waters (in Russian). *Bulletin of Science and Technology Information* 4, no. 16: 12–22 (Moscow: Gosgeoltekhizdat).

- Pitrak, M., S. Mares, and M. Kobr. 2007. A simple borehole dilution technique to measure horizontal ground water flow. *Ground Water* 45, no. 1: 89–92.
- Schwarz, R., T. Ptak, T. Holder, and G. Teutsch. 1998. Groundwater risk assessment at contaminated sites: A new approach for the inversion of contaminant concentration data measured at pumping wells. In *Groundwater Quality: Remediation and Protection*, Vol. 250, ed. M. Herbert, and K. Kovar, 68–71. Oxford, UK: IAHS Press.
- Swartjes, F.A. 2011. *Dealing with Contaminated Sites. From Theory Towards Practical Application*. Dordrecht/Heidelberg/London/New York: Springer.
- Vermeul, V.R., J.P. McKinley, D.R. Newcomer, R.D. Mackley, and J.M. Zachara. 2011. River-induced flow dynamics in long-screen wells and impact on aqueous samples. *Ground Water* 49, no. 4: 515–524.
- Verreydt, G., I. Van Keer, J. Bronders, L. Diels, and P. Vanderauwera. 2012. Flux-based risk management strategy of groundwater pollutions: The CMF approach. *Environmental Geochemistry and Health* 34, no. 6. DOI:10.1007/s10653-012-9491-x.
- Wu, Y.-S., C.-H. Lee, and Y.-L. Yu. 2008. Effects of hydraulic variables and well construction on horizontal borehole flowmeter measurements. *Ground Water Monitoring & Remediation* 28, no. 1: 64–74.